

Gravitino Dark Matter

Wilfried Buchmüller

Deutsches Elektronen-Synchrotron DESY, 22607 Hamburg, Germany

Abstract. Gravitino dark matter, together with thermal leptogenesis, implies an upper bound on the masses of superparticles. In the case of broken R-parity the constraints from primordial nucleosynthesis are naturally satisfied and decaying gravitinos lead to characteristic signatures in high energy cosmic rays. Electron and positron fluxes from gravitino decays cannot explain both, the PAMELA positron fraction and the electron + positron flux recently measured by Fermi LAT. The observed fluxes require astrophysical sources. The measured antiproton flux allows for a sizable contribution of decaying gravitinos to the gamma-ray spectrum, in particular a line at an energy below 300 GeV.

Keywords: supergravity, dark matter, leptogenesis, cosmic rays

PACS: 98.70.Sa, 95.35.+d

WHY GRAVITINO DARK MATTER?

An unequivocal prediction of locally supersymmetric extensions of the Standard Model is the gravitino, the gauge fermion of supergravity [1]. Its discovery would be of fundamental importance, as the discovery of the W- and Z-bosons for the electroweak theory. Depending on the mechanism of supersymmetry breaking, it can be the lightest superparticle (LSP), which makes it a natural dark matter candidate. So far, almost nothing is known about the gravitino mass. Examples of considered mass ranges are

- $m_{3/2} < 1$ keV, corresponding to hot dark matter [2],
- $1 \text{ keV} < m_{3/2} < 15 \text{ keV}$, representing warm dark matter [3],
- $100 \text{ keV} < m_{3/2} < 10 \text{ MeV}$, a range of cold dark matter, favoured by gauge mediation and thermal leptogenesis [4, 5],
- $100 \text{ GeV} < m_{3/2} < 1 \text{ TeV}$, a range of cold dark matter typical for gaugino and gravity mediation, suggested in connection with thermal leptogenesis [6].

It is very interesting that the various gravitino mass ranges are strongly correlated with the masses of other superparticles and with the history of the cosmological evolution. This leads to upper bounds on the gluino mass, lower and upper bounds on the next-to-lightest superparticle mass (NLSP) and also upper bounds on the reheating temperature in the early universe. Moreover, there is a close connection with baryogenesis.

It would be very exciting to discover a massive gravitino and to establish in this way spontaneously broken local supersymmetry as a fundamental, hidden symmetry of nature. This appears impossible for the most popular scenario of heavy gravitinos with neutralino LSP. On the contrary, it may be possible to discover a gravitino LSP which manifests itself as missing energy in NLSP decays [7, 8].

GRAVITINO PROBLEM OR VIRTUE?

In a supersymmetric plasma at high temperature gravitinos are thermally produced, mostly by QCD processes. Their number density $n_{3/2}$ increases linearly with the reheating temperature,

$$\frac{n_{3/2}}{n_\gamma} \propto \frac{\alpha_3}{M_p^2} T_R, \quad (1)$$

where M_p and α_3 are the Planck mass and the QCD fine structure constant, respectively. The late decay of heavy gravitinos alters the successful BBN prediction, which implies upper bounds for the reheating temperature T_R . The most stringent one from hadronic decays reads [9]

$$T_R < \mathcal{O}(1) \times 10^5 \text{ GeV}. \quad (2)$$

This is clearly incompatible with thermal leptogenesis [10] which leads to the lower bound $T_R \gtrsim 10^9 \text{ GeV}$ (cf. [11, 12]).

The conflict between the upper bound from BBN and the lower bound from leptogenesis on the reheating temperature can be avoided if the gravitino is the LSP [6]. In this case the BBN bounds apply to the NLSP which is quasi-stable. One also has to worry about gravitino dark matter which may overclose the universe.

In general, two processes contribute to the generation of gravitino dark matter. In the SuperWIMP mechanism [13, 14] gravitinos are produced in WIMP decays. The gravitino mass density is then determined by the NLSP density,

$$\Omega_{3/2} = \frac{m_{3/2}}{m_{\text{NLSP}}} \Omega_{\text{NLSP}}, \quad (3)$$

which is independent of the reheating temperature T_R . The BBN constraints require, however, rather large NLSP masses [15], which makes it difficult to test this mechanism at the LHC. The thermal production of gravitinos is dominated by $2 \rightarrow 2$ QCD scattering processes. Solving the Boltzmann equations one obtains [16, 17]

$$\Omega_{3/2} h^2 \simeq 0.5 \left(\frac{T_R}{10^{10} \text{ GeV}} \right) \left(\frac{100 \text{ GeV}}{m_{3/2}} \right) \left(\frac{m_{\tilde{g}}(\mu)}{1 \text{ TeV}} \right)^2, \quad (4)$$

where the two-loop running of the gluino mass from the reheating temperature to the electroweak scale has been taken into account [18]. It is remarkable that the observed dark matter density is obtained for typical SUSY breaking parameters, $m_{3/2} \sim 100 \text{ GeV}$, $m_{\tilde{g}} \sim 1 \text{ TeV}$ and a reheating temperature characteristic for leptogenesis, $T_R \sim \sqrt{m_{3/2} M_P} \sim 10^{10} \text{ GeV}$ [6].

The type and masses of NLSP's consistent with leptogenesis and gravitino dark matter are strongly restricted by constraints from BBN (cf. [19]), in particular by the catalyzed production of ${}^6\text{Li}$ in the case of a stau NLSP [20]. If the reheating process, which leads to the temperature T_R , is taken into account the constraints are sometimes relaxed. For instance, in the case of inflaton decays into right-handed neutrinos, $\phi \rightarrow N_1 N_1 \rightarrow (lH)(lH) \rightarrow \dots$, the reheating temperature required for leptogenesis is smaller by about one order of magnitude [21, 22]. If the Boltzmann equation for lepton asymmetry

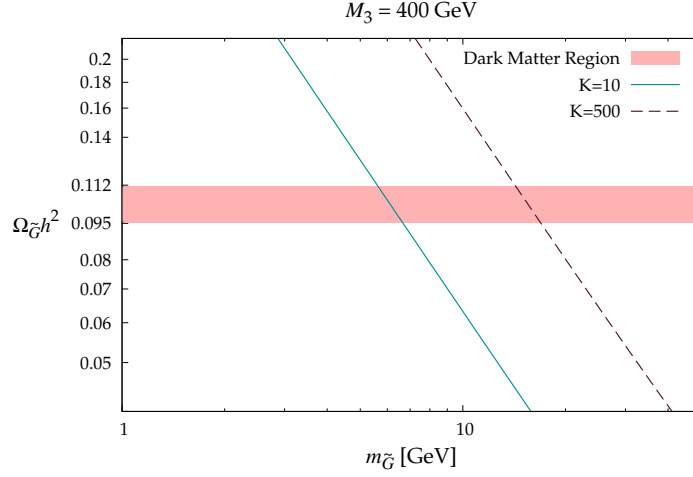


FIGURE 1. Relic gravitino density as function of the gravitino mass; the GUT scale parameter $M_3 = 400$ GeV corresponds to the on-shell gluino mass $m_{\tilde{g}} \simeq 1$ TeV. The leptogenesis parameters are $M_1 = 10^9$ GeV and K which lies in the ‘strong washout regime’. From [23].

and gravitino density are solved simultaneously, a connection between gravitino mass and neutrino parameters is obtained directly, without any reference to the reheating temperature. As an example (see Figure 1), for $M_1 = 10^9$ GeV, $K = 10$ ($\tilde{m}_1 = 0.01$ eV) and $m_{\tilde{g}} = 1$ TeV one finds $m_{3/2} \simeq 6$ GeV [23].

DECAYING GRAVITINO DARK MATTER

Nucleosynthesis, leptogenesis and gravitino dark matter can all be consistent in the case of a small R-parity breaking [24], which leads to the processes $\tilde{\tau}_R \rightarrow \tau \nu_\mu, \mu \nu_\tau, \tilde{\tau}_L \rightarrow b^c t, \dots$ and also to $\psi_{3/2} \rightarrow \gamma \nu$. Small R-parity breaking couplings can be induced by B-L breaking,

$$\lambda \sim h^{(e,d)} \Theta \lesssim 10^{-7}, \quad \Theta \sim \frac{v_{B-L}^2}{M_{\text{P}}^2}, \quad (5)$$

where $h^{(e,d)}$ are the lepton and down-quark Yukawa couplings, respectively. The ‘short’ NLSP lifetimes, e.g.,

$$c\tau_{\tilde{\tau}}^{\text{lep}} \sim 30 \text{ cm} \left(\frac{m_{\tilde{\tau}}}{200 \text{ GeV}} \right)^{-1} \left(\frac{\lambda}{10^{-7}} \right)^{-2}, \quad (6)$$

typically lead to NLSP decay before BBN. One finds that BBN, thermal leptogenesis and gravitino dark matter are consistent for $10^{-14} < \lambda, \lambda' < 10^{-7}$ and $m_{3/2} \gtrsim 5$ GeV [24]. Characteristic signals at the LHC can be strongly ionising macroscopic charged tracks, followed by a muon track, or a jet and missing energy, corresponding to $\tilde{\tau} \rightarrow \mu \nu_\tau$ and $\tilde{\tau} \rightarrow \tau \nu_\mu$, respectively.

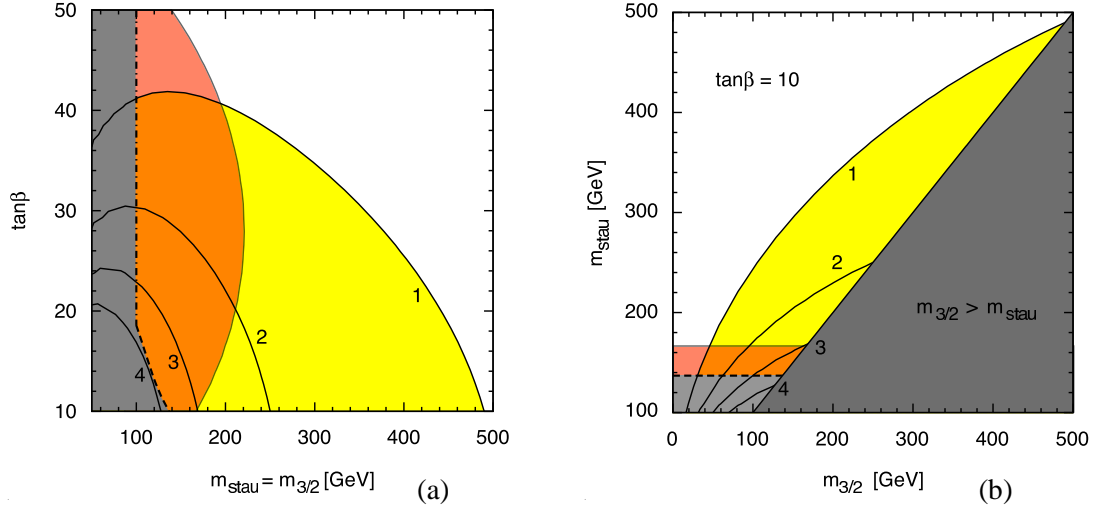


FIGURE 2. Boundary conditions (B) with stau NLSP. (a) Contours of constant reheating temperature, $T_R = (1 - 4) \times 10^9$ GeV, with $\Omega_{3/2} = \Omega_{\text{DM}}$ (solid lines); the gray region is excluded by constraints from low-energy experiments; thermal leptogenesis is possible in the yellow and orange regions; the orange region is favored by the muon $g - 2$ anomaly at the 2σ level. (b) Contours of constant reheating temperature in the $m_{\text{stau}} - m_{3/2}$ plane; in the dark gray region, the gravitino is not the LSP. From [18].

The gravitino decay $\psi_{3/2} \rightarrow \gamma\nu$ is suppressed both by the Planck mass and small R-parity breaking couplings, so that the lifetime is much longer than the age of the universe [25],

$$\tau_{3/2} \sim 10^{26} \text{ s} \left(\frac{\lambda}{10^{-7}} \right)^{-2} \left(\frac{m_{3/2}}{10 \text{ GeV}} \right)^{-3}. \quad (7)$$

Decaying dark matter with lifetime $\mathcal{O}(10^{26})$ s has become very popular after the recent observation of the rise in the cosmic-ray positron fraction by the PAMELA collaboration [26]. Note that R-parity breaking scenarios with gravitino lifetimes of this order can be realized in various ways [27, 28, 29, 30, 31].

The consistency of leptogenesis and gravitino dark matter implies important constraints on the superparticle mass spectrum, which depends on the boundary conditions of the supersymmetry breaking parameters at the grand unification (GUT) scale. Typical examples are

$$(A) \quad m_0 = m_{1/2}, \quad a_0 = 0; \quad (B) \quad m_0 = 0, \quad m_{1/2}, \quad a_0 = 0, \quad (8)$$

with a bino-like neutralino (A), and a right-handed stau (B) as NLSP, respectively. The corresponding upper bounds on the gravitino and stau masses are shown in Figure 2 for reheating temperatures in the range $T_R = (1 - 4) \times 10^9$ GeV [18]. Relaxing the boundary conditions at the GUT scale, gravitino masses up to 1.4 TeV are possible [32].

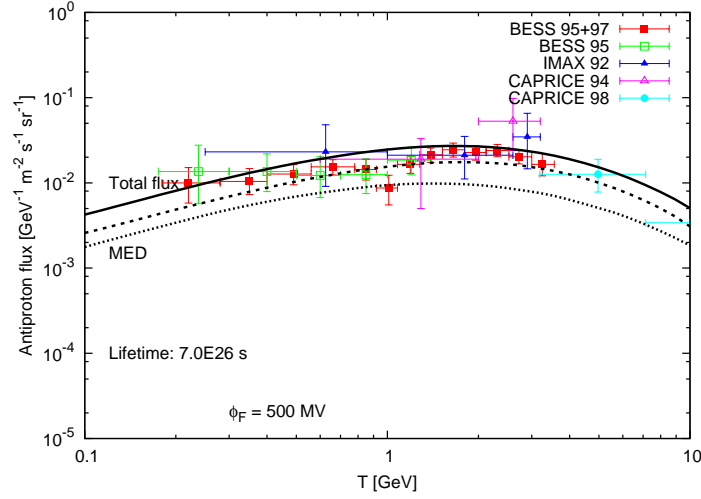


FIGURE 3. Antiproton flux for $m_{3/2} = 200$ GeV in the MED set of propagation parameters that saturate the antiproton overproduction bound. Dotted line: antiproton flux from gravitino decays, dashed line: secondary antiproton flux from spallation in the case of minimal nuclear cross section, solid line: total antiproton flux. The gravitino lifetime is $\tau_{3/2} = 7 \times 10^{26}$ s. From [34].

CONSTRAINTS FROM PAMELA AND FERMI

The R-parity violating gravitino decays $\psi_{3/2} \rightarrow \gamma\nu, h\nu, Z\nu, W^\pm l^\mp$ lead to interesting cosmic-ray signatures [33] which we shall discuss in the following in a model-independent way based on an operator analysis [34]. The mass scales multiplying the non-renormalizable operators are inverse powers of the Planck mass M_P and the supersymmetry breaking gravitino mass $m_{3/2}$. This assumes for the masses m_{SM} of Standard Model particles, the gravitino mass and the masses m_{soft} of other superparticles the hierarchy $m_{SM}^2 \ll m_{3/2}^2 \ll m_{soft}^2$. One easily verifies that the dimension-5 and dimension-6 operators for the R-parity violating couplings of the gravitino are given by

$$\mathcal{L}_{eff} = \frac{i\kappa}{\sqrt{2}M_P} \left\{ \bar{l}\gamma^\lambda \gamma^\nu D_\nu \phi \psi_\lambda + \frac{i}{2} \bar{l}\gamma^\lambda (\xi_1 g' Y B_{\mu\nu} + \xi_2 g W_{\mu\nu}) \sigma^{\mu\nu} \phi \psi_\lambda \right\} + \text{h.c.}, \quad (9)$$

where typically $\xi_{1,2} = \mathcal{O}(1/m_{3/2})$. Note, that in general κ and the product $\kappa\xi_{1,2}$ are independent parameters which depend on flavour.

The dimension-5 operator describes the processes $\psi_{3/2} \rightarrow h\nu, Z\nu, W^\pm l^\mp$ which, after fragmentation of Higgs, Z- and W-bosons, yields continuous gamma and antimatter spectra, $\psi_{3/2} \rightarrow \gamma X, \bar{p}X, e^+X$, which therefore are strongly correlated. It is remarkable that the decay $\psi_{3/2} \rightarrow \gamma\nu$ is controlled by the dimension-6 operator. Hence, the intensity of a line in the gamma-ray spectrum is not tied to the continuous part of the spectrum.

The interstellar antiproton flux from gravitino decay suffers from uncertainties in the determination of the physical parameters in the propagation of charged cosmic rays in the diffusive halo, leading to uncertainties in the magnitude of fluxes as large as two orders of magnitude at the energies relevant for present antiproton experiments. The requirement that the total antiproton flux from gravitino decay be consistent with

measurements gives a lower bound on the gravitino mass which strongly depends on the choice of the halo model. In the following we shall adopt the MED propagation model, which provides the best fit to the B/C ratio and measurements of flux ratios of radioactive cosmic-ray species [35].

A conservative upper bound on the antiproton flux from gravitinos is obtained by demanding that the total flux is not larger than the theoretical uncertainty band of the MED propagation model. This means that a ‘minimal’ dark matter lifetime for the MED model can be defined by a scenario where the secondary antiproton flux from spallation is 25% smaller than the central value, due to a putative overestimation of the nuclear cross sections, and the total antiproton flux saturates the upper limit of the uncertainty band which stems from astrophysical uncertainties discussed above.

Using this prescription one finds the lower bound on the gravitino lifetime $\tau_{3/2}^{\min} \simeq 7 \times 10^{26}$ s for $m_{3/2} = 200$ GeV. The corresponding antiproton flux from gravitino decay, the secondary antiproton flux from spallation and the total antiproton flux are shown in Figure 3 together with the experimental measurements by BESS, IMAX and WiZard/CAPRICE, and the uncertainty band from the nuclear cross sections in the MED propagation model. The minimal lifetime $\tau_{3/2}^{\min}$ can be compared with the gravitino lifetime needed to explain the PAMELA positron fraction excess.

It is now straightforward to calculate the positron flux at Earth from gravitino decay in the MED propagation model [35]. Note that the sensitivity of the positron fraction to the propagation model is fairly mild at the energies where the excess is observed, since these positrons are produced within a few kiloparsecs from the Earth and barely suffer the effects of diffusion.

To compare the predictions to the PAMELA results, we calculate the positron fraction, defined as the flux ratio $\Phi_{e^+}/(\Phi_{e^+} + \Phi_{e^-})$. For the background fluxes of primary and secondary electrons, as well as secondary positrons, we extract the fluxes from “Model 0” presented by the Fermi LAT collaboration in [36], which fits well the low energy data points of the total electron plus positron flux and the positron fraction, and is similar to the MED model for energies above a few GeV [37]. Then, the positron fraction reads

$$\text{PF}(T) = \frac{\Phi_{e^+}^{\text{DM}}(T) + \Phi_{e^+}^{\text{bkg}}(T)}{\Phi_{e^+}^{\text{DM}}(T) + \Phi_{e^+}^{\text{bkg}}(T) + \Phi_{e^-}^{\text{DM}}(T) + k \Phi_{e^-}^{\text{bkg}}(T)}, \quad (10)$$

where $k = \mathcal{O}(1)$ is the normalization of the astrophysical contribution to the primary electron flux, which is chosen to provide a qualitatively good fit to the data.

For the PAMELA positron excess to be due to gravitino dark matter decay, the gravitino mass must be at least 200 GeV. The decay $\psi_{3/2} \rightarrow W^\pm \ell^\mp$ then has a branching ratio of $\sim 50\%$, and the hard leptons that are directly produced in these decays may account for the rise in the positron fraction if a significant fraction of these leptons has electron or muon flavour.

Consider first the extreme case that the decays occur purely into electron flavour. For $m_{3/2} = 200$ GeV, the PAMELA excess can then be explained for the gravitino lifetime $\tau_{3/2}^e(200) \simeq 3.2 \times 10^{26}$ s, as illustrated by Figure 4. Note that this lifetime is a factor 2 smaller than the minimum lifetime which was obtained from the antiproton constraint. However, the MIN model and other sets of parameters that yield intermediate values

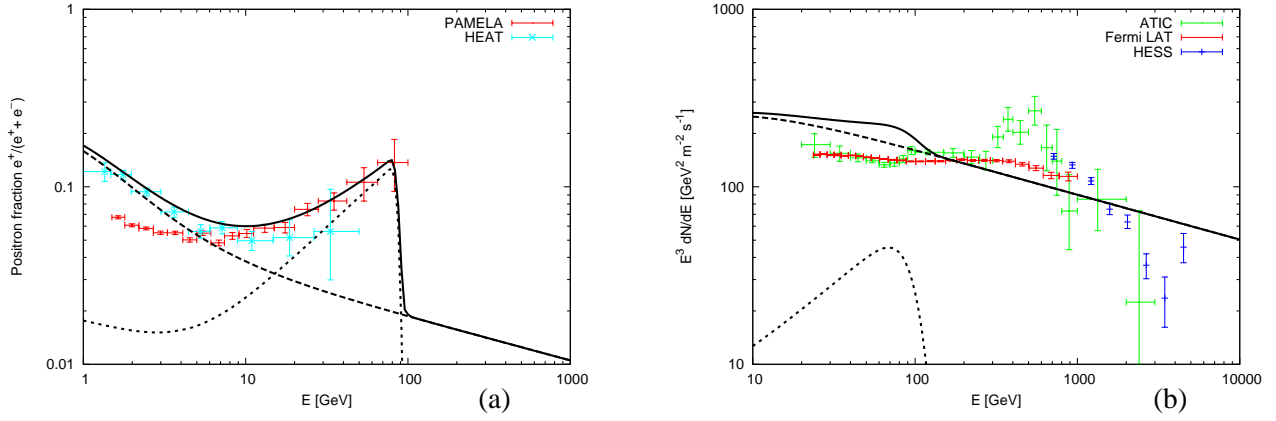


FIGURE 4. ‘Electron dominance’. Contribution from dark matter decay to the positron fraction (a), and the total electron + positron flux (b), compared with data from PAMELA and HEAT, and ATIC, Fermi LAT and HESS, respectively; $m_{3/2} = 200$ GeV, $\tau_{3/2} = 3.2 \times 10^{26}$ s; for $W^\pm l^\mp$ decays pure electron flavour is assumed. The “Model 0” [36] background is used, and for comparison with Fermi LAT data 25% energy resolution is taken into account. From [34].

for the antiproton flux can easily be compatible with both the positron fraction and the antiproton-to-proton ratio observed by PAMELA. The situation is very similar for $m_{3/2} = 400$ and 600 GeV.

Figure 4 also shows the predicted total electron + positron flux together with the results from Fermi LAT [39] and ATIC [40]. Obviously, the “Model 0” cannot account for the present data, and the contribution from gravitino decays makes the discrepancy even worse. In particular, the data show no spectral feature expected for decaying dark matter. On the other hand, gravitino decays may very well be consistent with the measured total electron + positron flux once the background is appropriately adjusted.

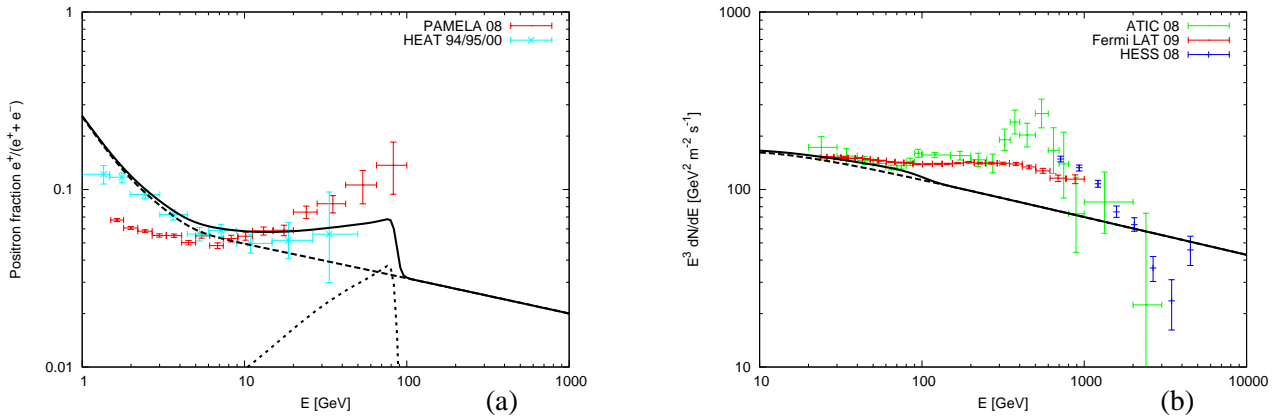


FIGURE 5. ‘Flavour democracy’. Contribution from dark matter decay to the positron fraction (a), and the total electron + positron flux (b), compared with data from PAMELA and HEAT, and ATIC, Fermi LAT and HESS, respectively; $m_{3/2} = 200$ GeV, with the minimal lifetime $\tau_{3/2} = 7 \times 10^{26}$ s; for $W^\pm l^\mp$ decays democratic flavour dependence is assumed. The “Model 0” [36] background is used, and for comparison with Fermi LAT data 25% energy resolution is taken into account. From [34].

This is evident from Figure 5 where the contribution from gravitino decays is shown in the theoretically well motivated case of flavour democratic decays. The figure also illustrates that, depending on the gravitino mass, the dark matter contribution to the PAMELA excess can still be significant.

An obvious possibility is that both, the total electron + positron flux and the positron fraction, are dominated by astrophysical sources. For instance, for the gravitino mass $m_{3/2} = 100$ GeV one obtains from the antiproton flux constraint the minimal lifetime $\tau_{3/2}^{\min}(100) \simeq 1 \times 10^{27}$ s. The corresponding contribution from gravitino decays to the total electron + positron flux and positron fraction turns out to be indeed negligible [34]. Nevertheless, as discussed in the next section, the dark matter contribution to the gamma-ray flux can still be sizable.

PREDICTIONS FOR THE GAMMA-RAY SPECTRUM

The gamma-ray flux from gravitino dark matter decay receives contributions from the decay of gravitinos in the Milky Way halo and at cosmological distances, which can be calculated in the standard manner. The halo component dominates, leading to a slightly anisotropic gamma-ray flux.

The gravitino decay produces a continuous spectrum of gamma-rays which is determined by the fragmentation of the Higgs boson and the weak gauge bosons. In addition, there exists a gamma-ray line at the endpoint of the spectrum with an intensity which is model-dependent. For our numerical analysis we use a typical branching ratio in this channel,

$$\text{RR}(\psi_{3/2} \rightarrow \nu\gamma) = 0.02 \left(\frac{200 \text{ GeV}}{m_{3/2}} \right)^2, \quad (11)$$

for gravitino masses above 100 GeV. In Figure 6 the predicted diffuse gamma-ray flux is shown for $m_{3/2} = 100, 200$ GeV and the respective lower bounds on the gravitino lifetime. These spectra correspond to upper bounds on the signal in gamma-rays that can be expected from gravitino dark matter decay.

For our analysis, two sets of results are used since the status of the extragalactic background is currently unclear. For the background obtained by Moskalenko et al., the extragalactic component is described by the power law [38]

$$\left[E^2 \frac{dJ}{dE} \right]_{\text{bg}} = 6.8 \times 10^{-7} \left(\frac{E}{\text{GeV}} \right)^{-0.32} (\text{cm}^2 \text{ str s})^{-1} \text{ GeV}. \quad (12)$$

The earlier analysis by Sreekumar et al. led to a less steep background [41],

$$\left[E^2 \frac{dJ}{dE} \right]_{\text{bg}} = 1.37 \times 10^{-6} \left(\frac{E}{\text{GeV}} \right)^{-0.1} (\text{cm}^2 \text{ str s})^{-1} \text{ GeV}. \quad (13)$$

In Figure 6, the slightly anisotropic halo signal has been averaged over the whole sky, excluding a band of $\pm 10^\circ$ around the Galactic disk. For the energy resolution $\sigma(E)/E = 15\%$ has been used.

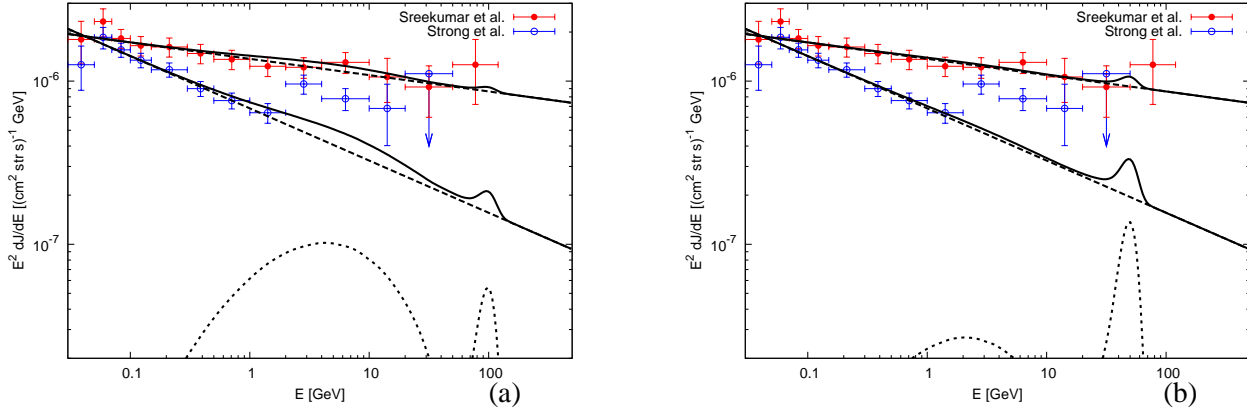


FIGURE 6. Gamma-ray flux for (a) $m_{3/2} = 200$ GeV, $\tau_{3/2}^{\min} = 7 \times 10^{26}$ s, and (b) $m_{3/2} = 100$ GeV, $\tau_{3/2}^{\min} = 1 \times 10^{27}$ s. The signal is added to two different backgrounds obtained in [38], [41]. From [34].

CONCLUSION

In supersymmetric theories with small R-parity breaking thermally produced gravitinos can account for the observed dark matter, consistent with leptogenesis and nucleosynthesis. Gravitino decays then contribute to antimatter cosmic rays as well as gamma-rays. Gravitino masses below 600 GeV are consistent with universal boundary conditions at the GUT scale.

Gravitino decays into Standard Model particles can be studied in a model-independent way by means of an operator analysis. For sufficiently large gravitino masses the dimension-5 operator dominates. This means that the branching ratios into $h\nu$, $Z\nu$ and $W^{\pm}l^{\mp}$ are fixed. As a consequence, the gamma-ray flux is essentially determined once the antiproton flux is known. On the contrary, the positron flux is model-dependent. The gamma-ray line is controlled by the dimension-6 operator. Its strength is model-dependent and decreases with increasing gravitino mass.

Electron and positron fluxes from gravitino decays cannot account for both, the PAMELA positron fraction and the electron + positron flux measured by Fermi LAT. For gravitino dark matter, the observed fluxes require astrophysical sources. However, depending on the gravitino mass, the dark matter contribution to the electron and positron fluxes can be non-negligible.

Present data on antiproton cosmic-rays allow for a sizable contribution of gravitino dark matter to the gamma-ray spectrum, in particular a line at an energy below 300 GeV. Non-observation of such a line would place a lower bound on the gravitino lifetime, and hence on the strength of R-parity breaking, restricting possible signatures at the LHC.

ACKNOWLEDGMENTS

This talk is based on recent work with A. Ibarra, M. Endo, T. Shindou, F. Takayama and D. Tran whom I thank for a fruitful collaboration.

REFERENCES

1. D. Z. Freedman, P. van Nieuwenhuizen and S. Ferrara, Phys. Rev. D **13** (1976) 3214; S. Deser and B. Zumino, Phys. Lett. B **62** (1976) 335.
2. H. Pagels and J. R. Primack, Phys. Rev. Lett. **48** (1982) 223.
3. D. Gorbunov, A. Khmelnitsky and V. Rubakov, JHEP **0812** (2008) 055 [0805.2836 [hep-ph]].
4. M. Fujii, M. Ibe and T. Yanagida, Phys. Rev. D **69** (2004) 015006 [hep-ph/0309064].
5. J. J. Heckman, A. Tavanfar and C. Vafa, 0812.3155 [hep-th].
6. M. Bolz, W. Buchmuller and M. Plumacher, Phys. Lett. B **443** (1998) 209 [hep-ph/9809381].
7. G. F. Giudice and R. Rattazzi, Phys. Rept. **322** (1999) 419 [hep-ph/9801271].
8. W. Buchmuller, K. Hamaguchi, M. Ratz and T. Yanagida, Phys. Lett. B **588** (2004) 90 [hep-ph/0402179].
9. M. Kawasaki, K. Kohri and T. Moroi, Phys. Lett. B **625**, 7 (2005) [astro-ph/0402490]; K. Jedamzik, Phys. Rev. D **74**, 103509 (2006) [hep-ph/0604251].
10. M. Fukugita and T. Yanagida, Phys. Lett. B **174**, 45 (1986).
11. S. Davidson and A. Ibarra, Phys. Lett. B **535** (2002) 25 [hep-ph/0202239].
12. W. Buchmuller, P. Di Bari and M. Plumacher, Annals Phys. **315**, 305 (2005) [hep-ph/0401240].
13. L. Covi, J. E. Kim and L. Roszkowski, Phys. Rev. Lett. **82** (1999) 4180 [hep-ph/9905212].
14. J. L. Feng, A. Rajaraman and F. Takayama, Phys. Rev. Lett. **91** (2003) 011302 [hep-ph/0302215].
15. J. L. Feng, S. Su and F. Takayama, Phys. Rev. D **70** (2004) 075019 [hep-ph/0404231].
16. M. Bolz, A. Brandenburg and W. Buchmuller, Nucl. Phys. B **606** (2001) 518 [Erratum-ibid. B **790** (2008) 336] [hep-ph/0012052].
17. J. Pradler and F. D. Steffen, Phys. Rev. D **75** (2007) 023509 [hep-ph/0608344].
18. W. Buchmuller, M. Endo and T. Shindou, JHEP **0811** (2008) 079 [0809.4667 [hep-ph]].
19. F. D. Steffen, Eur. Phys. J. C **59** (2009) 557 [0811.3347 [hep-ph]].
20. M. Pospelov, Phys. Rev. Lett. **98** (2007) 231301 [hep-ph/0605215].
21. T. Asaka, K. Hamaguchi, M. Kawasaki and T. Yanagida, Phys. Lett. B **464** (1999) 12 [hep-ph/9906366].
22. F. Hahn-Woernle and M. Plumacher, Nucl. Phys. B **806** (2009) 68 [0801.3972 [hep-ph]].
23. M. Erbe, DESY THESIS 2009
24. W. Buchmuller, L. Covi, K. Hamaguchi, A. Ibarra and T. Yanagida, JHEP **0703**, 037 (2007) [hep-ph/0702184].
25. F. Takayama and M. Yamaguchi, Phys. Lett. B **485**, 388 (2000) [hep-ph/0005214].
26. O. Adriani *et al.* [PAMELA Collaboration], Nature **458** (2009) 607 [0810.4995 [astro-ph]].
27. S. Lola, P. Osland and A. R. Raklev, Phys. Lett. B **656** (2007) 83 [0707.2510 [hep-ph]].
28. X. Ji, R. N. Mohapatra, S. Nussinov and Y. Zhang, Phys. Rev. D **78** (2008) 075032 [0808.1904 [hep-ph]].
29. M. Endo and T. Shindou, JHEP **0909** (2009) 037 [0903.1813 [hep-ph]].
30. K. Y. Choi, D. E. Lopez-Fogliani, C. Munoz and R. R. de Austri, 0906.3681 [hep-ph].
31. P. Fileviez Perez and S. Spinner, these proceedings.
32. K. Hamaguchi, F. Takahashi and T. T. Yanagida, Phys. Lett. B **677** (2009) 59 [0901.2168 [hep-ph]].
33. D. Tran, these proceedings.
34. W. Buchmuller, A. Ibarra, T. Shindou, F. Takayama and D. Tran, JCAP **0909** (2009) 021 [0906.1187 [hep-ph]].
35. D. Maurin, F. Donato, R. Taillet and P. Salati, [astro-ph/0101231].
36. D. Grasso *et al.* [FERMI-LAT Collaboration], Astropart. Phys. **32** (2009) 140 [0905.0636 [astro-ph.HE]].
37. T. Delahaye, F. Donato, N. Fornengo, J. Lavalle, R. Lineros, P. Salati and R. Taillet, 0809.5268 [astro-ph].
38. A. W. Strong, I. V. Moskalenko and O. Reimer, Astrophys. J. **613**, 956 (2004); Astrophys. J. **613** (2004) 962 [astro-ph/0406254].
39. A. A. Abdo *et al.* [The Fermi LAT Collaboration], Phys. Rev. Lett. **102** (2009) 181101 [0905.0025 [astro-ph.HE]].
40. J. Chang *et al.*, Nature **456** (2008) 362.
41. P. Sreekumar *et al.* [EGRET Collaboration], Astrophys. J. **494** (1998) 523 [astro-ph/9709257].